Geostrophic Shock Waves

DORON NOF

Department of Oceanography, The Florida State University, Tallahassee, FL 32306

(Manuscript received 1 July 1985, in final form 4 November 1985)

ABSTRACT

Organized depth discontinuities involving a balance between steepening and dissipation are usually referred to as shock waves. An analytical "reduced gravity" model is used to examine a special kind of shock wave. The wave under study is a depth discontinuity associated with a transition between a supercritical and subcritical flow in a channel. Even though the wave itself is highly nonlinear, the adjacent upstream and downstream fields are exactly geostrophic in the cross-stream direction. For this reason we term the wave a geostrophic shock wave. We focus on a stationary shock wave whose horizontal projection is a straight line perpendicular to the side walls. Solutions for the entire field are constructed analytically using power series expansions and shock conditions equivalent to the so-called Rankine-Hugoniot constraints.

It is found that, for particular upstream conditions, a geostrophic shock wave can be formed if the particle speed exceeds the surface gravity wave speed (i.e., the flow is "supercritical"). Specifically, in addition to supercriticality, a stationary geostrophic wave requires the upstream velocity to have a particular structure which depends on the strength of the shock and the channel width. When the latter condition is not met, a shock wave is still possible, but its adjacent fields will not be geostrophic and its shape will correspond to an "S" rather than a straight line.

Being the only known analytical solution for the entire field of shock waves on a rotating earth, the geostrophic shock provides useful information on the wave structure. For instance, it is shown that even though momentum is conserved across the shocks, relatively large changes in potential vorticity take place. *For depth discontinuity of O(1) (i.e., high "amplitudes"), there is a generation of potential vorticity that is also of O(1).* Such a phenomenon does not occur on a nonrotating plane where the (zero) potential vorticity is always conserved across shocks.

The above considerations imply that the oceanic potential vorticity may be altered through the action of shock waves in channels and passages. Possible application of this theory to various oceanic situations is mentioned.

1. Introduction

The occurrence of shock waves in nonrotating river flows is well studied and documented (e.g., Lighthill, 1978; Stoker, 1957). The shock can be either propagating ("tidal bore") or stationary and is associated with a sudden and violent change in depth accompanied by a local energy loss. It is generated when a shallow *supercritical* flow (i.e., a flow with a speed greater than the gravity wave propagation rate) suddenly "jumps" into a deeper, less energetic *subcritical* flow (i.e., a flow with a speed smaller than the gravity wave propagation rate).

Many oceanic channels have flows with particle speeds exceeding the Kelvin wave speed [e.g., the Mediterranean outflow (Armi and Farmer, 1985), the flow in the Vema Channel (Hogg, 1983)]. It is, therefore, desirable to extend the known theories for nonrotating channels to large-scale flows subject to the influence of the earth's rotation. Having such a unified theory at hand may help to explain the sudden depth changes observed in the lee of various sills [e.g., the Denmark Strait (Bainbridge, 1976, page 9)].

The development of a unified theory for shock waves[1] is not at all straightforward, because once rotation is introduced to the problem, the number of directions along which there are nonzero pressure gradients increases from one to two (Figs. 1 and 2). Namely, the problem is not only highly nonlinear, it is also two-dimensional. We shall see that despite these difficulties, it is possible to obtain analytical solutions for rotating shocks; before describing them in more detail, however, it is useful to discuss some previous, related work.

The most closely related work is the numerical solutions of Pratt (1983), which address shock waves generated by the presence of a sill in a rotating channel.

[1] Many authors do not discriminate between a depth discontinuity on a nonrotating plane and a discontinuity on an *f*-plane and term both phenomena a hydraulic jump. While this is certainly acceptable, the author prefers to use the expression shock wave, jump or bore for such phenomena on a rotating earth. This is because the traditional use of the word *hydraulic* has been mainly reserved for *manmade* structures (*The Oxford English Dictionary*, 1971, s.v. "hydraulic") which are relatively small. As a point of general interest, it is mentioned that the word *hydraulic* was originally used in Greek to describe a kind of musical instrument played by means of water.

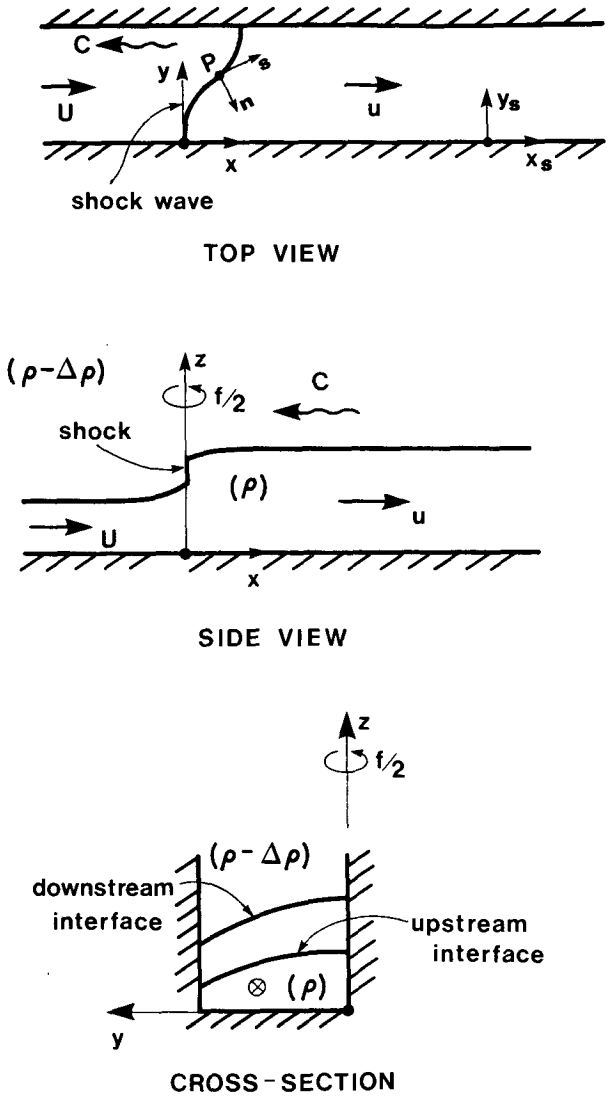

FIG. 1. A schematic diagram of a rotational shock wave in a rectangular channel. The current is flowing underneath an infinitely deep passive layer. The stationary coordinates are x_s and y_s; x and y are the coordinates in a system moving with the shock. The coordinates n and s are normal and tangential to the shock; they correspond to a pure rotation of the moving coordinate system at P. Solid arrows denote flow direction and "wiggly" arrows denote propagation.

Pratt's (1983) analysis, which considers a flow touching both channel walls, has demonstrated that (i) the presence of rotation does not prevent the initiation and generation of shock waves, and (ii) the jumps are formed in a similar fashion to nonrotating shocks. An additional closely related study is that of Nof (1984) who considered shock waves in a separated current (i.e., a flow touching only one of the channel walls). In that study, shocks resulting from a sudden increase in the upstream depth (and transport) have been examined analytically by connecting the far upstream and downstream fields without solving for the immediate vicinity of the shock.

There are two important differences between the Nof (1984) study and the geostrophic shock considered in the present paper. The first difference is associated with the fact that in the separated current the direct connection between the far upstream and far downstream fields implies that it is necessary to adopt a closure condition on the speed or the potential vorticity. For the channel case, on the other hand, we shall find solutions for the entire field so that no closure condition will be necessary. The second difference between the two investigations is that, in the separated case, the shocks must always be moving, whereas in the channel case, the shocks can also be stationary.

In addition to the investigations mentioned above, there have been a number of numerical studies which examined the evolution of rotating shock waves in the atmosphere. Among these studies are those of Houghton and Kasahara (1968), Houghton (1969), Williams and Hori (1970) and Parrett and Cullen (1984). While these investigations are informative, they do not deal directly with the problem considered in this paper—where a supercritical geostrophic flow "jumps" to a subcritical geostrophic flow. With these investigations in mind, we shall return now to our discussion of the geostrophic shock.

The particular approach that we shall use to solve for the geostrophic shock can be described as follows. We shall apply the nonlinear shallow water equations for a layer and a half. Friction will be neglected everywhere except within the shock itself. Across the shock, momentum and mass are conserved and conditions similar to the so-called Rankine–Hugoniot constraints are to be satisfied. These conditions imply that energy must be lost within the shock and that potential vorticity may or may not be conserved. Three points should be made regarding the potential vorticity. First, Yamagata (1980) argues that potential vorticity can be

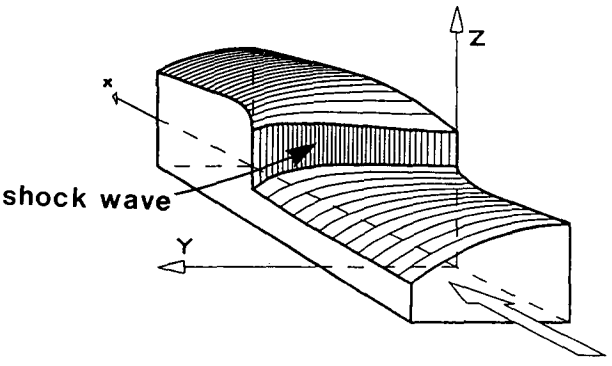

FIG. 2. A schematic three-dimensional view of the rotational shock wave shown in Fig. 1. Note that there are two transition zones in the immediate vicinity of the shock; one corresponds to an adjustment of the upstream unidirectional flow to the two-dimensional shock, and the other is a readjustment to a unidirectional flow downstream (see Fig. 3a).

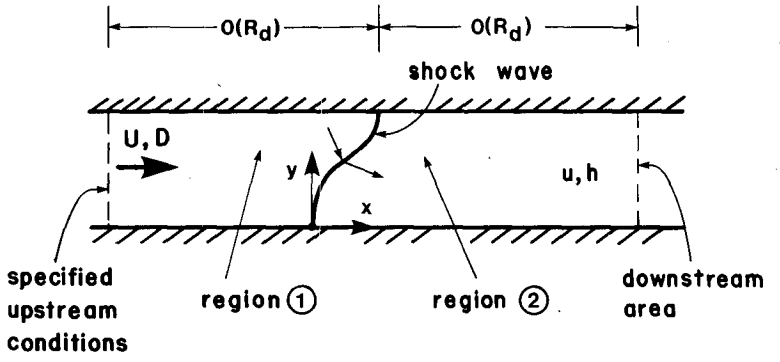

FIG. 3a. A detailed view of a shock wave in a rotating channel and its neighboring transition zones. The upstream flow U adjusts in region 1 to a two-directional flow and the associated S-shaped shock; the fluid crosses the shock without any sliding as shown by the two small solid arrows. In region 2, the fluid readjusts to a unidirectional downstream state (u). Note that the length scale of the transition zone is the deformation radius. The channel width is smaller than the deformation radius so that the interface always intersects the side walls.

conserved across rotating shocks. Nof (1984) being, at the time, unaware of Yamagata's study, has also suggested that in a separated current, potential vorticity is probably conserved. Second, Pratt (1983) has numerically found that, in some of his experiments, there are very small changes in the potential vorticity across the shocks. Third, we shall see that, surprisingly, geostrophic shocks of O(1) involve a *large increase* in the potential vorticity.

Particular attention will be given to stationary shock waves (i.e., waves whose propagation tendency has been arrested by advection), and we shall see that even for such relatively simple shocks the solution is quite complicated. Instead of specifying the upstream conditions and deriving the downstream flow and the shock shape, which is the traditional procedure for such problems, we shall specify the shock shape and derive the appropriate conditions upstream and downstream. We shall see that, in general, as pointed out by Pratt (1983), a shock in a channel has an "S" shape (Figs. 1, 2 and 3) which is perpendicular to the channel walls. Hence, the general problem of a rotating shock wave in a channel involves a region where the flow across the channel can be as large as the flow along the channel. Namely, the flow in the immediate vicinity of the shock is not necessarily geostrophic.

For our case, we *choose* the shock shape to be a straight line and the flow to be unidirectional everywhere. This implies that, even in the immediate vicinity of the shock, the upstream and downstream flows are exactly geostrophic in the cross-channel direction (Fig. 4). The above is demonstrated analytically using the relationships associated with conservation of mass and momentum across the shock and a power series expansion in ϵ, the ratio between the channel width and the Rossby deformation radius. Much of the discussion

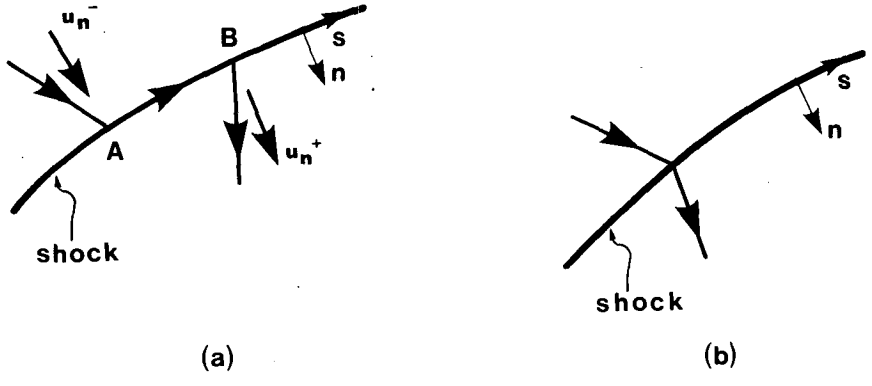

FIG. 3b. Schematic diagram of sliding along the shock (a). Such a situation is impossible because $u_n^+ = u_n^- = 0$ along section AB so that by (2.1) $h^+ = h^-$ (along AB) meaning that there is no shock. Consequently, particles can only change their direction as they cross the shock (b). Adapted from Nof (1984).

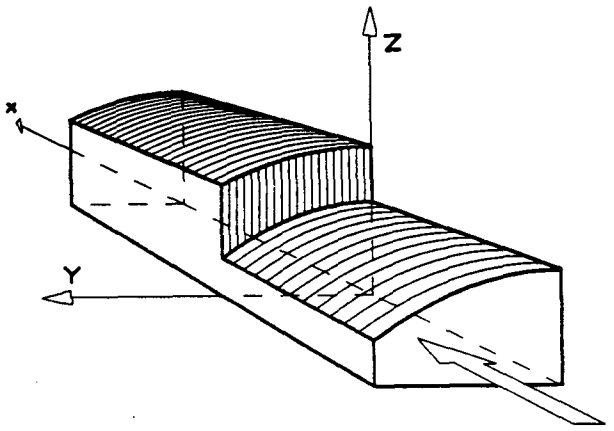

FIG. 4. A schematic three-dimensional view of the geostrophic shock wave. In contrast to the more general shock shown in Figs. 1, 2 and 3a, the geostrophic shock is a straight line (perpendicular to the channel walls) free from adjacent transition zones; the flow is unidirectional and geostrophic everywhere.

is devoted to a detailed examination of the change in potential vorticity across the shock. After presenting this analysis, we shall consider an application of the theory to the deep water flow in (i) the Windward Passage, (ii) the Vema Channel and (iii) the Denmark Strait. Several observations suggest that, in these channels, stationary shock waves may be present.

This paper is organized as follows. We begin by formulating the problem for a steadily translating shock (section 2) and discussing the shock conditions. We then present the general solution for a geostrophic shock which follows directly from the shock conditions (section 3) and proceed with a presentation of the asymptotic expansion and the detailed solution (section 4). The analysis of the solution is given in section 5 and our results are discussed and summarized in section 6.

2. Formulation

Consider again the system shown in Figs. 1, 2 and 3. An inviscid current with a density (ρ) is flowing underneath an infinitely deep fluid with a density ($\rho - \Delta\rho$) [or on top of an infinitely deep current with a density ($\rho + \Delta\rho$) (not shown)]. We shall consider two main coordinate systems, a fixed coordinate system whose axes (x_s and y_s) are directed along and across the channel, and a coordinate system traveling with the shock (x, y). Both systems rotate uniformly at $f/2$ about the vertical axis (z). We seek the conditions under which the current's upper interface can somewhere "jump" to a higher or lower depth. Namely, we are looking for the properties of the current which will allow a depth discontinuity to occur. In general, the shock can be propagating upstream or downstream because of the two walls. Note that, as mentioned earlier, in this respect the behavior is very different from that of the separated shock considered by Nof (1984) where only downstream propagation is possible.

For the general problem, the upstream conditions are given; namely, the speed U and the depth D are known. As pointed out by Pratt (1983) and Nof (1984), the Rankine–Hugoniot conditions for shocks on a rotating earth are

$$h^+(u_n^+)^2 + \frac{g'}{2}(h^+)^2 = h^-(u_n^-)^2 + \frac{g'}{2}(h^-)^2 \quad (2.1)$$

$$h^+u_n^+u_s^+ = h^-u_n^-u_s^- \quad (2.2)$$

$$h^+u_n^+ = h^-u_n^- \quad (2.3)$$

where n and s are coordinates normal and tangential to the shock at some point (P) (Fig. 1), the minus and plus superscripts denote that the variable in question is associated with cross sections behind ($n = -\xi$, $\xi \to 0$) and ahead ($n = \xi$, $\xi \to 0$) of the shock, u_n and u_s are the normal and tangential velocities at P, g' is the "reduced gravity" ($g\Delta\rho/\rho$), and h is the depth. Note that (2.1)–(2.3) were obtained by integrating the momentum and continuity equations *across the shock* so that they correspond to a local balance at all points along the shock. Also, note that the conservation of momentum across the shock essentially implies that the force of the flow on the two sides of the shock is identical. This must be the case, unless the shock has a finite width and there is some kind of bottom stress. For a general discussion of the conservation of momentum and mass across shocks see, for example, Courant and Friedrichs (1948), Stoker (1957) and Lighthill (1978).

A number of comments should be made regarding (2.1)–(2.3). First, note that (2.1)–(2.3) are valid only for a steadily moving shock and that u_n and u_s are the speeds as viewed from a moving coordinate system. Second, it is worth mentioning that since (2.1)–(2.3) are associated with a simple rotation of the moving coordinate system (Pratt, 1983; Nof, 1984), u_n and u_s are the normal and tangential velocities measured at various points along the shock. They differ from the normal and tangential speeds frequently used in natural coordinate systems whose origin is located at a fixed point along a given curve. Third, it should be pointed out that (2.1)–(2.2) correspond to conservation of momentum across the shock, whereas (2.3) reflects the conservation of mass. Fourth, as pointed out by Pratt (1983), a shock in a rotating channel must be perpendicular to the channel walls. Also, as shown by Nof (1984), no sliding along the shock can take place because sliding implies that $u_n^+ = u_n^- = 0$ along some section along the shock. Such a situation is impossible because for $u_n^- = u_n = 0$, (2.1) implies that there is no shock (see Fig. 3b). Finally, for each particle, the energy loss across the shock is

$$G^- - G^+ = g'(h^+ - h^-)^3/4h^-h^+ \quad (2.4)$$

where $G = g'h + u^2/2$ is the Bernoulli function. Note that G is the energy of a particle so that the total energy flux is huG. Since $h^+u^+ = h^-u^-$, the total energy loss is $hu(G^- - G^+)$. As shown by Pratt (1983), the change in the potential vorticity is,

$$K^+ - K^- = \frac{\partial s}{\partial \psi}\left[\left(\frac{dG}{ds}\right)^+ - \left(\frac{dG}{ds}\right)^-\right] \quad (2.5a)$$

where the stream function ψ is defined by

$$\frac{\partial \psi}{\partial s} = -u_n h; \quad \frac{\partial \psi}{\partial n} = u_s h. \quad (2.5b)$$

Relation (2.4) implies that there must always be an energy loss within the shock and that particles should always enter the shock from the low depth area and emerge at the larger depth region. On the other hand, (2.5a) indicates that potential vorticity is not necessarily lost nor is it necessarily conserved across the shock. We shall see later that for our geostrophic shocks there will actually be a relatively large *gain* in the potential vorticity.

Relations (2.1)–(2.5a) indicate that the general problem of a shock wave in a rotating channel consists of a curve with an S shape across which there is an energy loss. The flow in the vicinity of the shock is two-dimensional in the sense that there are variations in depth across the channel [i.e., $h = h(x, y)$] and the cross-channel velocities are of the same order as the long channel speed (see Fig. 3). In addition to these complications, the general problem is, obviously, nonlinear because the abrupt depth changes across the shock give rise to an important contribution from the nonlinear terms [see (2.1)].

To solve the general problem, one needs to find the shock shape and propagation speed for given upstream conditions. This procedure involves matching of two transition zones—the upstream and downstream regions (adjacent to the shock) where an adjustment from a unidirectional flow to two directional flows is taking place (Fig. 3). The equations for these regions are the usual shallow water equations, so that we have

$$u_i \frac{\partial u_i}{\partial x} + v_i \frac{\partial u_i}{\partial y} - fv_i + g' \frac{\partial h_i}{\partial x} = 0 \quad (2.6)$$

$$u_i \frac{\partial v_i}{\partial x} + v_i \frac{\partial v_i}{\partial y} + f(u_i + C) + g' \frac{\partial h_i}{\partial y} = 0 \quad (2.7)$$

$$\frac{\partial}{\partial x}(h_i u_i) + \frac{\partial}{\partial y}(h_i v_i) = 0 \quad (2.8)$$

where $i = 1, 2$ correspond to the upstream transition zone and the downstream transition zone, f is the Coriolis parameter, u_i and v_i are the velocity components in the x and y direction, and C is the propagation rate.

The complete problem consists, then, of finding the solution in the two transition zones with the shock conditions providing the matching conditions. Because of the nonlinearity and the need to find the shape of the shock as part of the problem, the general case appears (to the author) to be intractable analytically. For this reason, we shall simplify the general problem and take the following approach.

Instead of specifying the upstream conditions and looking for the shock shape and the solutions for the transition zones, we shall specify the shock shape and then look for the associated upstream conditions. We shall consider the simplest possible shock shape which satisfies the shock conditions—a straight line perpendicular to the channel walls. In addition, we shall require the velocity to be parallel to the channel walls everywhere (see Fig. 4). These simplifications eliminate the need to calculate the shock shape but, more importantly, they also eliminate the existence of the transition zones (see Fig. 3a) because whatever the flow a distance ξ (where $\xi \to 0$) upstream of shock is, it can be extended to the far upstream area. Requiring the shock shape to be a straight line perpendicular to the channel walls, and the flow to be unidirectional, implies that the flow is geostrophic everywhere (except inside the shock, where the flow is unspecified).

In addition to these simplifications, we shall focus our attention on stationary shocks, i.e., shocks whose propagation tendency has been arrested by advection. One can visualize various situations that can lead to such a state. For example, if an obstacle is suddenly introduced into a supercritical flow, then a shock wave which propagates upstream will be generated. This upstream propagation can be arrested if the upstream flow is as fast as the shock speed. We shall see in the next section that the above simplifications enable one to construct analytically tractable solutions.

3. Governing equations for the geostrophic shock

a. The simplified shock conditions

For a unidirectional flow with a shock whose projection on the x, y plane is a straight line (i.e., $u_s^+ = u_s^- = 0$), the shock conditions (2.1)–(2.3) reduce to

$$DU^2 + g'D^2/2 = hu^2 + g'h^2/2 \quad (3.1)$$

$$DU = hu \quad (3.2)$$

where all the variables are now a function of y alone [i.e., $D = D(Y)$, $U = U(y)$, $h = h(y)$, and $u = u(y)$]. Since our upstream and downstream fields are not a function of x, we have, for simplicity, changed our notation in such a way that U and D denote the speed and depth for all $x \leq 0$ (see Fig. 4) and u and h are the speed and depth for $x \geq 0$. It is important to note that, although the general distribution of U and D is unknown, the upstream conditions near the wall [i.e., $D(0)$, $U(0)$] are given.

For convenience, we introduce the following nondimensional variables:

$$\left.\begin{aligned} &\hat{U} = U/U(0); \quad \hat{u} = u/U(0); \\ &\hat{D} = D/D(0); \quad \hat{h} = h/D(0); \\ &\mathrm{Fr} = U(0)/[g'D(0)]^{1/2}; \quad \mathrm{Ro} = U(0)/fb \end{aligned}\right\} \tag{3.3}$$

where Fr and Ro are the Froude and Rossby numbers and b is the channel width.

In terms of (3.3), the simplified shock conditions (3.1)–(3.2) are

$$\mathrm{Fr}^2\hat{D}(\hat{U})^2 + (\hat{D})^2/2 = \mathrm{Fr}^2\hat{h}(\hat{u})^2 + (\hat{h})^2/2 \tag{3.4}$$

$$\hat{D}\hat{U} = \hat{u}\hat{h}. \tag{3.5}$$

Elimination of $\hat{u}$ between (3.4) and (3.5) gives,

$$(\hat{h} - \hat{D})\left[\frac{1}{2}(\hat{h})^2 + \frac{\hat{D}}{2}\hat{h} - \mathrm{Fr}^2\hat{D}(\hat{U})^2\right] = 0. \tag{3.6}$$

Similarly, elimination of $\hat{h}$ between (3.4) and (3.5) gives,

$$(\hat{u} - \hat{U})[\mathrm{Fr}^2\hat{U}\hat{D}(\hat{u})^2 - \hat{u}(\hat{D})^2/2 - (\hat{D})^2\hat{U}/2] = 0. \tag{3.7}$$

The nontrivial solutions of (3.6) and (3.7) satisfying the condition of $\hat{h} > 0$, are

$$\boxed{\hat{h} = \{[(\hat{D})^2 + 8\ \mathrm{Fr}^2\hat{D}(\hat{U})^2]^{1/2} - \hat{D}\}/2} \tag{3.8}$$

$$\boxed{\hat{u} = \{\hat{D} + [(\hat{D})^2 + 8\ \mathrm{Fr}^2\hat{D}(\hat{U})^2]^{1/2}\}/4\ \mathrm{Fr}^2\hat{U}.} \tag{3.9}$$

For an energy loss to occur within the shock, we must require $\hat{h} > \hat{D}$ [by (2.4)] which, together with (3.8), gives the criticality condition

$$[(\hat{D})^2 + 8\ \mathrm{Fr}^2\hat{D}(\hat{U})^2]^{1/2} \geqslant 3\hat{D}$$

or

$$\boxed{\mathrm{Fr}^2 \geqslant \hat{D}/(\hat{U})^2.} \tag{3.10}$$

This relationship implies that, in order for a shock to occur, the "local" Froude number $U(y)/[g'D(y)]^{1/2}$ must be larger than unity *everywhere* across the channel. Namely, it must be larger than unity for *all* y. Note that for $\hat{D} = \hat{U} = 1$ [i.e., no variations across the channel, or equivalently, no rotation ($f = 0$)], (3.8), (3.9) and (3.10) reduce to the familiar relationships for nonrotating jumps (e.g., see Stoker, 1957),

$$\hat{h} = [(1 + 8\ \mathrm{Fr}^2)^{1/2} - 1]/2 \tag{3.11a}$$

$$\hat{u} = [1 + (1 + 8\ \mathrm{Fr}^2)^{1/2}]/4\ \mathrm{Fr}^2. \tag{3.11b}$$

b. The geostrophic shock

So far we have only used the shock conditions; i.e., we have taken into account that the shock shape is a straight line and that the flow is unidirectional everywhere. However, the variables must also satisfy the field equations (2.6)–(2.8), which for a unidirectional flow reduce to the geostrophic relationships,

$$\frac{\mathrm{Fr}^2}{\mathrm{Ro}}\hat{u} = -\frac{\partial\hat{h}}{\partial\hat{y}} \tag{3.12a}$$

$$\frac{\mathrm{Fr}^2}{\mathrm{Ro}}\hat{U} = -\frac{\partial\hat{D}}{\partial\hat{y}}. \tag{3.12b}$$

By taking the derivative of (3.8) with respect to y, considering (3.9) and (3.12) one can form a single differential equation for the upstream depth,

$$\epsilon^4(\hat{D})^2 + 8\epsilon^2\hat{D}\left(\frac{\partial\hat{D}}{\partial\hat{y}}\right)^2 + \epsilon\left[\epsilon^2(\hat{D})^2 + 8\hat{D}\left(\frac{\partial\hat{D}}{\partial\hat{y}}\right)^2\right]^{1/2}\left[\epsilon^2\hat{D} + 2\left(\frac{\partial\hat{D}}{\partial\hat{y}}\right)^2\right] - \frac{\partial\hat{D}}{\partial\hat{y}}\left\{2\epsilon^2\hat{D}\frac{\partial\hat{D}}{\partial\hat{y}} + 8\left[\left(\frac{\partial\hat{D}}{\partial\hat{y}}\right)^3 + 2\hat{D}\left(\frac{\partial\hat{D}}{\partial\hat{y}}\right)\frac{\partial^2\hat{D}}{\partial\hat{y}^2}\right]\right\} = 0 \tag{3.13a}$$

where we have introduced a new nondimensional variable,

$$\epsilon = \mathrm{Fr}/\mathrm{Ro} = b/R_d. \tag{3.13b}$$

Hence, ϵ measures the strength of the rotation or, equivalently, the width of the channel. Note that, so far, no approximations have been made so that (3.13a) is the exact governing equation for the geostrophic shock. In addition, note that, usually, $\epsilon \leqslant 1$ because otherwise (i.e., $\epsilon > 1$) the flow would intersect the floor rather than the side wall.

Equation (3.13) is subject to the boundary conditions,

$$\hat{D} = 1; \qquad \hat{y} = 0 \tag{3.14a}$$

$$\frac{\partial\hat{D}}{\partial\hat{y}} = -\epsilon\ \mathrm{Fr}; \quad \hat{y} = 0 \tag{3.14b}$$

which state that the depth and speed at the right wall are given. In addition to (3.14), the solution should satisfy,

$$\hat{D} > 0; \quad 0 \leqslant \hat{y} \leqslant 1$$

$$\hat{U} > 0; \quad 0 \leqslant \hat{y} \leqslant 1$$

which state that the depth is always positive and that there is no negative flow.

In the next section, we shall introduce a power series expansion in ϵ; since ϵ can easily reach values as high as 0.5 for many oceanic channels, we shall include high order terms in our expansion.

4. Asymptotic expansion

To solve (3.13), we assume that the solution possesses a power series expansion in ϵ,

$$\hat{D} = 1 + \epsilon D^{(1)} + \epsilon^2 D^{(2)} + \epsilon^3 D^{(3)} + \cdots \tag{4.1}$$

$$\hat{U} = 1 + \epsilon U^{(1)} + \epsilon^2 U^{(2)} + \cdots, \tag{4.2}$$

where the basic state (i.e., $\epsilon \to 0$) corresponds to no rotation or, equivalently, a channel with an infinitesimal width ($b \to 0$).

The relationship between (4.1) and (4.2) is found by expanding the geostrophic relationship,

$$\hat{U} = -\frac{1}{\epsilon\,\mathrm{Fr}}\frac{\partial \hat{D}}{\partial \hat{y}},$$

which gives

$$\epsilon + \epsilon^2 U^{(1)} + \epsilon^3 U^{(2)} + \cdots = -\frac{1}{\mathrm{Fr}}\left(\epsilon\frac{\partial \hat{D}^{(1)}}{\partial \hat{y}} + \epsilon^2\frac{\partial D^{(2)}}{\partial \hat{y}} + \epsilon^3\frac{\partial D^{(3)}}{\partial \hat{y}} + \cdots\right). \quad (4.3)$$

In addition, our variables should satisfy the upstream wall conditions (3.14), which imply

$$D^{(1)}(0) = D^{(2)}(0) = D^{(3)}(0) = \cdots = 0; \quad \hat{y} = 0$$
$$U^{(1)}(0) = U^{(2)}(0) = U^{(3)}(0) = \cdots = 0; \quad \hat{y} = 0. \quad (4.4)$$

Substitution of (4.1) into our general differential equation for the upstream field (3.13) shows that the O(1) terms are automatically satisfied and that there are no terms of O(ϵ) or O(ϵ^2).

The O(ϵ^3) balance is,

$$\frac{\partial D^{(1)}}{\partial \hat{y}}\left[\frac{\partial D^{(1)}}{\partial \hat{y}}\frac{\partial^2 D^{(1)}}{\partial \hat{y}^2}\right] = 0. \quad (4.5)$$

The solution satisfying (4.5) as well as the O(ϵ) terms in (4.3) and the boundary condition (4.4) is

$$D^{(1)} = -\mathrm{Fr}\hat{y}. \quad (4.6)$$

With the aid of (4.6), we find that the O(ϵ^4) balance of (3.13) is

$$1 + 6\,\mathrm{Fr}^2 + (1 + 8\,\mathrm{Fr}^2)^{1/2}(1 + 2\,\mathrm{Fr}^2) - 8\,\mathrm{Fr}^4 - 16\,\mathrm{Fr}^2\frac{\partial^2 D^{(2)}}{\partial \hat{y}^2} = 0. \quad (4.7)$$

Similarly, one finds that the O(ϵ^5) balance is

$$-2\,\mathrm{Fr}\hat{y} - 6\,\mathrm{Fr}\left[2\frac{\partial D^{(2)}}{\partial \hat{y}} + \mathrm{Fr}^2\hat{y}\right] + (1 + 8\,\mathrm{Fr}^2)^{1/2}\left[-\mathrm{Fr}\hat{y} - 4\,\mathrm{Fr}\frac{\partial D^{(2)}}{\partial \hat{y}} + \frac{A_1}{2}(1 + 2\,\mathrm{Fr}^2)\right] + 32\,\mathrm{Fr}^3\frac{\partial D^{(2)}}{\partial \hat{y}} - 16\left\{\frac{\partial^2 D^{(2)}}{\partial \hat{y}^2}\left[-2\,\mathrm{Fr}\frac{\partial D^{(2)}}{\partial \hat{y}} + \mathrm{Fr}^2 y\right] + \mathrm{Fr}^2\frac{\partial^2 D^{(3)}}{\partial \hat{y}^2}\right\} = 0, \quad (4.8)$$

and the O(ϵ^6) is found to be

$$(\mathrm{Fr}^2\hat{y} + 2D^{(2)}) + 6\left[-\mathrm{Fr}\left(2\frac{\partial D^{(3)}}{\partial \hat{y}} - \mathrm{Fr}D^{(2)}\right) + \frac{\partial D^{(2)}}{\partial \hat{y}}\left(2\,\mathrm{Fr}^2\hat{y} + \frac{\partial D^{(2)}}{\partial \hat{y}}\right)\right]$$
$$\times (1 + 8\,\mathrm{Fr}^2)^{1/2}\left\{\left(\frac{A_2}{2} - \frac{A_1^2}{8}\right)(1 + 2\,\mathrm{Fr}^2) + A_1\left(-\frac{\mathrm{Fr}\hat{y}}{2} - 2\,\mathrm{Fr}\frac{\partial D^{(2)}}{\partial \hat{y}}\right) + D^{(2)} + 2\left(\frac{\partial D^{(2)}}{\partial \hat{y}}\right)^2 - 4\,\mathrm{Fr}\frac{\partial D^{(3)}}{\partial \hat{y}}\right\}$$
$$- 8\,\mathrm{Fr}^2\left[\left(-4\,\mathrm{Fr}\frac{\partial D^{(3)}}{\partial \hat{y}}\right) + 6\left(\frac{\partial D^{(2)}}{\partial \hat{y}}\right)^2\right] - 16\left\{\frac{\partial^2 D^{(2)}}{\partial \hat{y}^2}\left[\frac{\partial D^{(2)}}{\partial \hat{y}}\left(\frac{\partial D^{(2)}}{\partial \hat{y}} + 2\,\mathrm{Fr}^2\hat{y}\right) - \mathrm{Fr}\left(-D_2\,\mathrm{Fr} + 2\frac{\partial D^{(3)}}{\partial \hat{y}}\right)\right]\right.$$
$$\left. + \frac{\partial^2 D^{(3)}}{\partial \hat{y}^2}\left[-2\,\mathrm{Fr}\frac{\partial D^{(2)}}{\partial \hat{y}} - \mathrm{Fr}^3\hat{y}\right] + \mathrm{Fr}^2\frac{\partial^2 D^{(4)}}{\partial \hat{y}^2}\right\} = 0 \quad (4.9)$$

where the functions A_1 and A_2 are given by

$$A_1 = \left\{-2\,\mathrm{Fr}\hat{y} + 8\left[-2\,\mathrm{Fr}\frac{\partial D^{(2)}}{\partial \hat{y}} - \mathrm{Fr}^3\hat{y}\right]\right\}\Big/(1 + 8\,\mathrm{Fr}^2) \quad (4.10a)$$

$$A_2 = \left\{\mathrm{Fr}^2\hat{y}^2 + 2D^{(2)} + 8\left[\left(\frac{\partial D^{(2)}}{\partial \hat{y}}\right)^2 - 2\,\mathrm{Fr}\frac{\partial D^{(3)}}{\partial \hat{y}} + 2\,\mathrm{Fr}^2\hat{y}\frac{\partial D^{(2)}}{\partial \hat{y}} + \mathrm{Fr}^2 D^{(2)}\right]\right\} \times (1 + 8\,\mathrm{Fr}^2)^{-1}. \quad (4.10b)$$

Note that, as mentioned earlier, the high order terms are needed because in the actual ocean ϵ can easily reach values as high as 0.5.

While being algebraically involved, the solutions of the above equations are straightforward and one ultimately finds

$$\hat{D} = 1 - \epsilon\,\mathrm{Fr}\hat{y} + \epsilon^2 A_3\hat{y}^2/2 + \epsilon^3 A_4\hat{y}^3/6 + \epsilon^4 A_5\hat{y}^4/12 + \cdots \quad (4.11)$$

$$\hat{U} = 1 - \epsilon A_3\hat{y}/\mathrm{Fr} - \epsilon^2 A_4\hat{y}^2/2\,\mathrm{Fr} - \epsilon^3 A_5\hat{y}^3/3\,\mathrm{Fr} + \cdots. \quad (4.12)$$

The functions A_3, A_4 and A_5 are given by

$$A_3 = [1 + 8\,\mathrm{Fr}^2 + (1 + 8\,\mathrm{Fr}^2)^{1/2}(1 + 2\,\mathrm{Fr}^2) - 2\,\mathrm{Fr}^2(1 + 4\,\mathrm{Fr}^2)]/16\,\mathrm{Fr}^2 \quad (4.13a)$$

$$A_4 = \{-(1 + 2\,\mathrm{Fr}^2)(1 + 4\,\mathrm{Fr}^2 + 8A_3) + 2(1 + 8\,\mathrm{Fr}^2)^{1/2}[16A_3^2 + 6A_3(4\,\mathrm{Fr}^2 - 1) - (3\,\mathrm{Fr}^2 + 1)] - (1 + 8\,\mathrm{Fr}^2)(1 + 4A_3)\}/16\,\mathrm{Fr}(1 + 8\,\mathrm{Fr}^2)^{1/2} \quad (4.13b)$$

$$A_5 = \{\mathrm{Fr}^2 + A_3(1 + 15\,\mathrm{Fr}^2) + 2A_3^2(3 - 44\,\mathrm{Fr}^2) - 16A_3^3 + 2A_4\,\mathrm{Fr}(16\,\mathrm{Fr}^2 - 3) + 48A_3A_4\,\mathrm{Fr} + (1 + 8\,\mathrm{Fr}^2)^{1/2}[(A_6 - A_7^2)(1 + 2\,\mathrm{Fr}^2)/2 + A_3(1 + 8\,\mathrm{Fr}A_6)/2 + 2(A_3^2 - \mathrm{Fr}A_4) + \mathrm{Fr}A_6]\}/16 \quad (4.13c)$$

where

$$A_6 = \mathrm{Fr}(1 + 8A_3 + 4\,\mathrm{Fr}^2)/(1 + 8\,\mathrm{Fr}^2) \quad (4.13d)$$

$$A_7 = [8A_3^2 + (20\,\mathrm{Fr}^2 + 1)A_3 + \mathrm{Fr}^2 - 8\,\mathrm{Fr}A_4]/(1 + 8\,\mathrm{Fr}^2). \quad (4.13e)$$

Relations (4.11)–(4.13) provide the desired solution for the upstream field ($x \leq 0$). The downstream ($x > 0$) variables $\hat{u}$, $\hat{h}$ are related to the upstream variables $\hat{U}$, $\hat{D}$ via the exact expressions (3.8) and (3.9) so that the entire field is now known. The meaning and implication of our asymptotic solutions are discussed in detail in the following section.

5. Analysis

With the aid of our approximate solution we shall now examine the various properties of the geostrophic shock.

a. The critical condition

Substitution of the solution (4.11)–(4.13) into (3.10) shows that the critical condition is

$$\mathrm{Fr}^2(1 - \epsilon A_2\hat{y}/\mathrm{Fr} - \epsilon^2 A_4\hat{y}^2/2\,\mathrm{Fr} - \epsilon^3 A_5\hat{y}^3/3\,\mathrm{Fr})^2 = 1 - \epsilon\,\mathrm{Fr}\hat{y} + \epsilon^2 A_3\hat{y}^2/2 + \epsilon^3 A_4\hat{y}^3/6 + \cdots$$

which, by equating like powers of ϵ, gives

$$\mathrm{Fr}^2 - 1 = 0 \quad (5.1a)$$

$$1 - 2A_3 = 0 \quad (5.1b)$$

$$A_3^2 - \mathrm{Fr}A_4 - A_3/2 = 0 \quad (5.1c)$$

$$A_3A_4/2 - 2A_5\,\mathrm{Fr}/A_4 - A_4/6 = 0. \quad (5.1d)$$

It is easy to show that (5.1b)–(5.1d) give an equality for $\mathrm{Fr}^2 = 1$. Namely, up to $O(\epsilon^3)$, the critical condition is given by $\mathrm{Fr} = 1$. Since Fr is computed on the basis of the variables near the right wall, it is not representative of the whole current. In view of this, we follow Gill (1977) and introduce a rotational Froude number ($\overline{F}_r$) which is computed on the basis of the algebraic averages of the depth and velocity (i.e., $\overline{F}_r = [\hat{U}(0) + \hat{U}(1)]/\{2[\hat{D}(0) + \hat{D}(1)]\}^{1/2}$). Note that this rotational Froude number is introduced merely for convenience; it represents an approximate ratio between the actual mean flow to the actual mean Kelvin wave speed. The relationship between the rotational Froude number ($\overline{F}_r$) and the Froude number based on the parameters near the wall (Fr) is shown in Fig. 5. With the aid of this relationship, one finds that the critical condition as a function of $\overline{F}_r$ is

$$\overline{F}_r = 1 - \epsilon^2/32 - \epsilon^3/64 + O(\epsilon^4). \quad (5.2)$$

This functional dependence is shown in Fig. 6. It suggests that the stationary shock can exist even if the linearly averaged flow velocity is smaller than the linearly averaged Kelvin wave speed. Recall, however, that the exact condition for the existence of a shock is that the "local" Froude number (i.e., $U(y)/[g'D(y)]^{1/2}$) be larger than unity for all y (Eq. 3.10) so that (5.2) does not really imply that the earth's rotation lowers the speed associated with criticality. All it means is that when one linearly averages the properties across the channel in the manner suggested by Gill (1977), one obtains a criticality condition corresponding to a new Froude number that is smaller than unity. Before proceeding and discussing the change in potential vorticity across the shock, it is instructive to illustrate the changes in velocity and depth. This is shown in Fig. 7, which displays their sensitivity to the Froude number; as expected, the strength of the shock increases as Fr increases.

b. The change of potential vorticity across the shock

To examine the difference between the potential vorticity on the two sides of the shock, we introduce the nondimensional potential vorticity,

$$\hat{K}_u = K_u/[f/D(0)]; \quad \hat{K}_d = K_d/[f/D(0)] \quad (5.3)$$

where the subscripts u and d denote the upstream ($x \leq 0$) and downstream ($x > 0$). Hence, we have

$$\hat{K}_u = \left(1 + \frac{1}{\epsilon^2}\frac{\partial^2\hat{D}}{\partial\hat{y}^2}\right)\Big/\hat{D} \quad (5.4a)$$

$$\hat{K}_d = \left(1 + \frac{1}{\epsilon^2}\frac{\partial^2\hat{h}}{\partial\hat{y}^2}\right)\Big/\hat{h} \quad (5.4b)$$

which, in view of (4.11)–(4.13), give

$$\hat{K}_u = (1 + A_3) + \epsilon[A_4 + \mathrm{Fr}(1 + A_3)]\hat{y} + \epsilon^2[A_5 + \mathrm{Fr}A_4 + (1 + A_3)(\mathrm{Fr}^2 - A_3/2)]\hat{y}^2 + O(\epsilon^3) \quad (5.5)$$

$$\hat{K}_d = \frac{2}{[(1 + 8\,\mathrm{Fr}^2)^{1/2} - 1]} \times \left\{A_8 - \epsilon\left[\frac{A_8[\mathrm{Fr} - A_6(1 + 8\,\mathrm{Fr}^2)^{1/2})]}{(1 + 8\,\mathrm{Fr}^2)^{1/2} - 1} + A_{10}/2\,\mathrm{Fr}\right]\hat{y} + \epsilon^2\left[A_8A_9 + \frac{A_{10}[\mathrm{Fr} - (1 + 8\,\mathrm{Fr}^2)^{1/2}A_6]}{2\,\mathrm{Fr}[(1 + 8\,\mathrm{Fr}^2)^{1/2} - 1]} - 3A_{11}/4\,\mathrm{Fr}\right]\hat{y}^2 + O(\epsilon^3)\right\}. \quad (5.6)$$

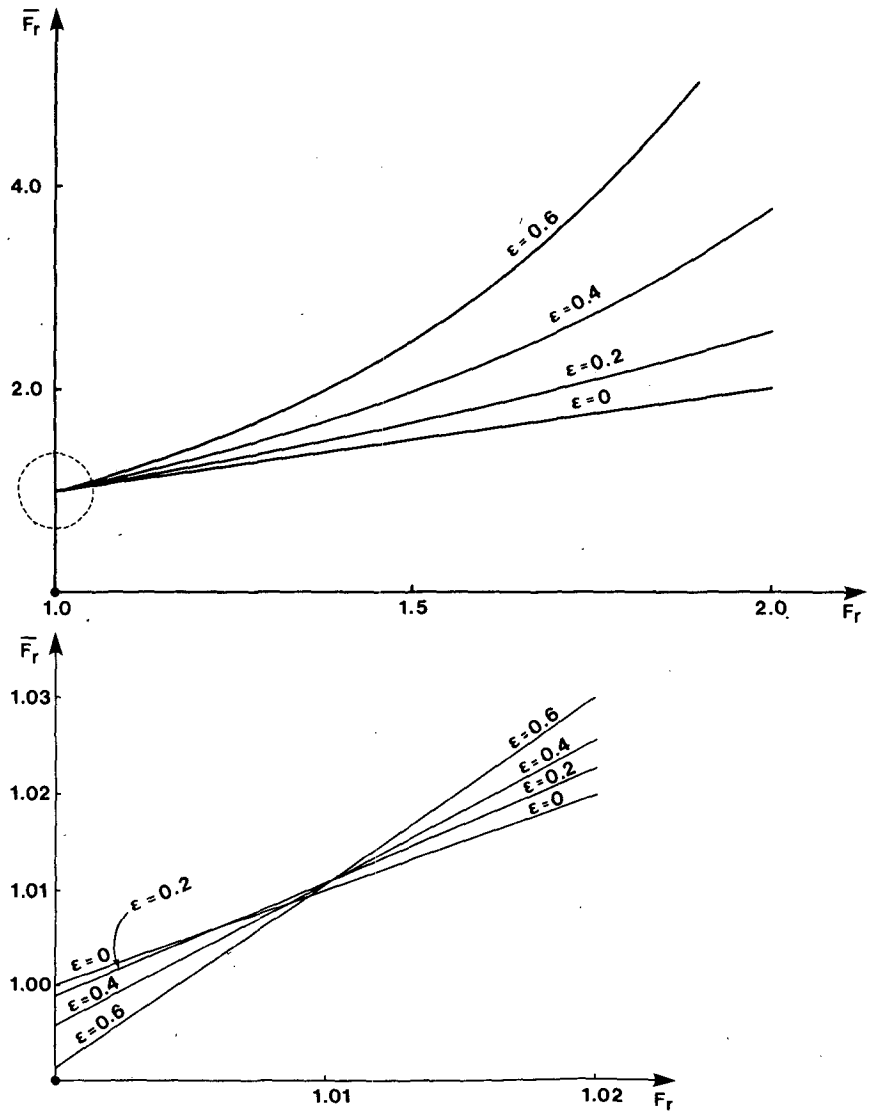

FIG. 5. The dependence of the rotational Froude number ($\overline{F}_r$) on the local Froude number (i.e., the Froude number which is based on the flow near the right wall). Note that $\overline{F}_r = [\hat{U}(0) + \hat{U}(1)]/\{2[\hat{D}(0) + \hat{D}(1)]\}^{1/2}$. The upper panel shows the functional dependence for $1 < \mathrm{Fr} < 2$; the lower panel is a "close-up" of the region bounded by the dashed circle.

The functions A_8, A_9, A_{10} and A_{11} are given by

$$A_8 = 1 + \frac{1}{4\,\mathrm{Fr}}\{A_6(1 + 8\,\mathrm{Fr}^2)^{1/2} + \mathrm{Fr} - [1 + (1 + 8\,\mathrm{Fr}^2)^{1/2}]A_3/\mathrm{Fr}\}$$

$$A_9 = \frac{A_3 - (1 + 8\,\mathrm{Fr}^2)^{1/2}(A_1 - A_6^2)}{2[(1 + 8\,\mathrm{Fr}^2)^{1/2} - 1]} + \frac{[\mathrm{Fr} - (1 + 8\,\mathrm{Fr}^2)^{1/2}A_6]^2}{[(1 + 8\,\mathrm{Fr}^2)^{1/2} - 1]^2}$$

$$A_{10} = \tfrac{1}{2}[(1 + 8\,\mathrm{Fr}^2)^{1/2}(A_7 - A_6^2) + A_3] - [\mathrm{Fr} + A_6(1 + 8\,\mathrm{Fr}^2)^{1/2}]A_3/\mathrm{Fr} + [1 + (1 + 8\,\mathrm{Fr}^2)^{1/2}][A_3^2/\mathrm{Fr}^2 + A_4/2\,\mathrm{Fr}]$$

$$A_{11} = [(1 + 8\,\mathrm{Fr}^2)^{1/2}(A_{12} + A_6A_7 - A_1^3)/2 + A_4/6] + [(1 + 8\,\mathrm{Fr}^2)^{1/2}(A_7 - A_6^2) + A_3]A_3/2\,\mathrm{Fr} - [\mathrm{Fr} + A_6(1 + 8\,\mathrm{Fr}^2)^{1/2}][A_3^2/\mathrm{Fr}^2 + A_4/2\,\mathrm{Fr}] + [1 + (1 + 8\,\mathrm{Fr}^2)^{1/2}]\left[\frac{A_3}{\mathrm{Fr}^2}\left(\frac{A_3^2}{\mathrm{Fr}} + A_4\right) + A_5/3\,\mathrm{Fr}\right]$$

where,

$$A_{12} = [-\mathrm{Fr}A_3(1 + 16A_3) + \frac{A_4}{3}(1 + 28\,\mathrm{Fr}^2) + 8A_3A_4 - 16\,\mathrm{Fr}A_5/3]/(1 + 8\,\mathrm{Fr}^2).$$

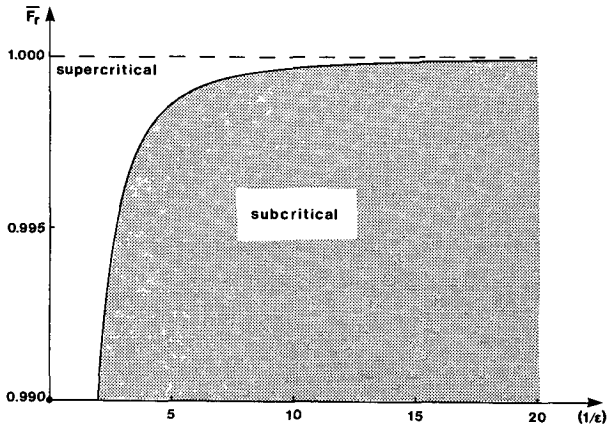

FIG. 6. The subcritical and supercritical regimes for a stationary geostrophic shock wave in a channel. The curve separating the two regions (i.e., the critical condition) is given by $\overline{F_r} = 1 - \epsilon^2/32 - \epsilon^3/64 + O(\epsilon^4)$.

The distribution of the potential vorticity upstream and downstream is shown in Fig. 8 and is illustrated in Figs. 9 and 10. The modifications in shear are shown in Fig. 11. Note that the fluid *gains* potential vorticity and gains shear as it crosses the shock. The gain in potential vorticity is of O(1) for shocks whose depth change (amplitude) is O(1). For weak shocks (i.e., shocks with small amplitude), the change of potential vorticity is minute. In fact, it is possible to show that if the depth change across the shock is, say, δ (where $\delta \ll 1$) then the change of potential vorticity across the shock is $O(\delta^2)$. Before proceeding, it is worth mentioning that the relationship between "upstream influence" and the modification of potential vorticity discussed by Nof (1984) has no bearing on the shock wave under study. This is because, in contrast to the separated case, the present shock is stationary, so that all the fluid always passes through the shock.

6. Summary and conclusions

The foregoing analysis, which leads to the steady solutions for the stationary geostrophic shock, was based on the following assumptions. First, it was assumed that, as in other kinds of shock waves, only momentum and mass are conserved across the shock. Second, it was assumed that friction and dissipation are confined to an infinitesimal region associated with the shock itself; in this area, energy is lost and potential vorticity can be altered. Instead of specifying the upstream conditions and solving for the shock (and its shape), which is the common procedure for such problems, we have specified the shock shape and found the corresponding upstream and downstream conditions. We focused our attention on shocks whose horizontal projection is a straight line perpendicular to the channel walls; the flow adjacent to the shock is geostrophic in the cross-stream direction. The properties of these shocks can be summarized as follows:

1) When a unidirectional channel flow with a particular velocity profile exceeds the speed of a Kelvin wave at all points across the channel, a stationary geostrophic shock wave can be formed.

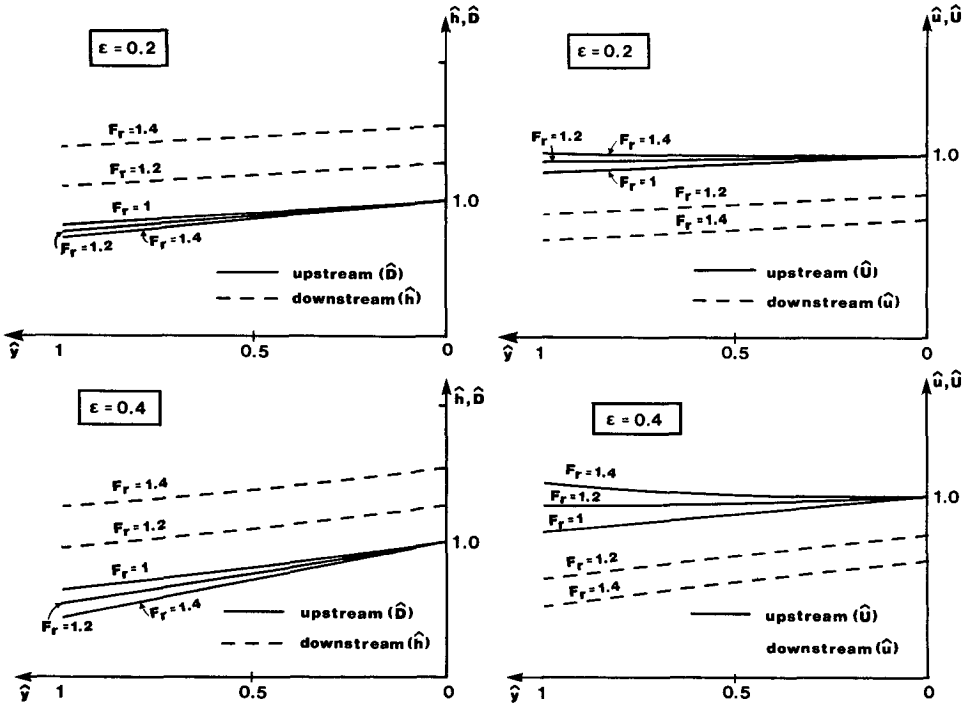

FIG. 7. The sensitivity of the upstream and downstream (left panels) and velocity (right panels) to the Froude number (Fr) and the channel width ($\epsilon = b/R_d$).

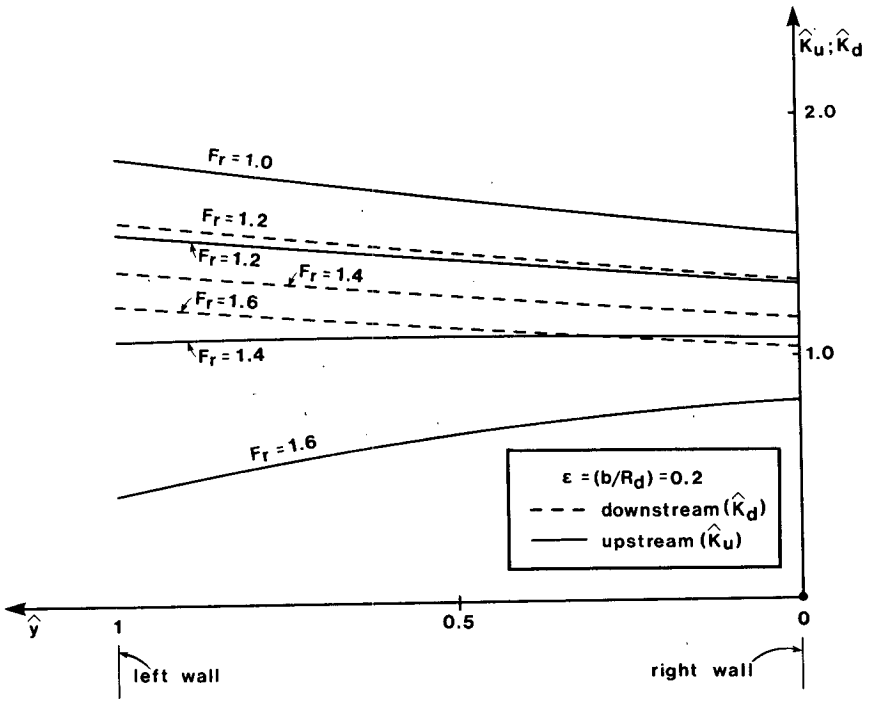

FIG. 8. The dependence of the upstream and downstream potential vorticity ($\hat{K}_u$ and $\hat{K}_d$, respectively) on the location and Froude number.

2) The flow is unidirectional and geostrophic *everywhere* except within the shock itself. *The largest wave amplitude is on the left-hand side.*

3) *Although there is an energy loss within the shock, there is a potential vorticity gain across the jump.* Namely, despite the fact that there is an increase in depth, the potential vorticity is larger downstream than it is upstream. For highly nonlinear shock waves (i.e.,

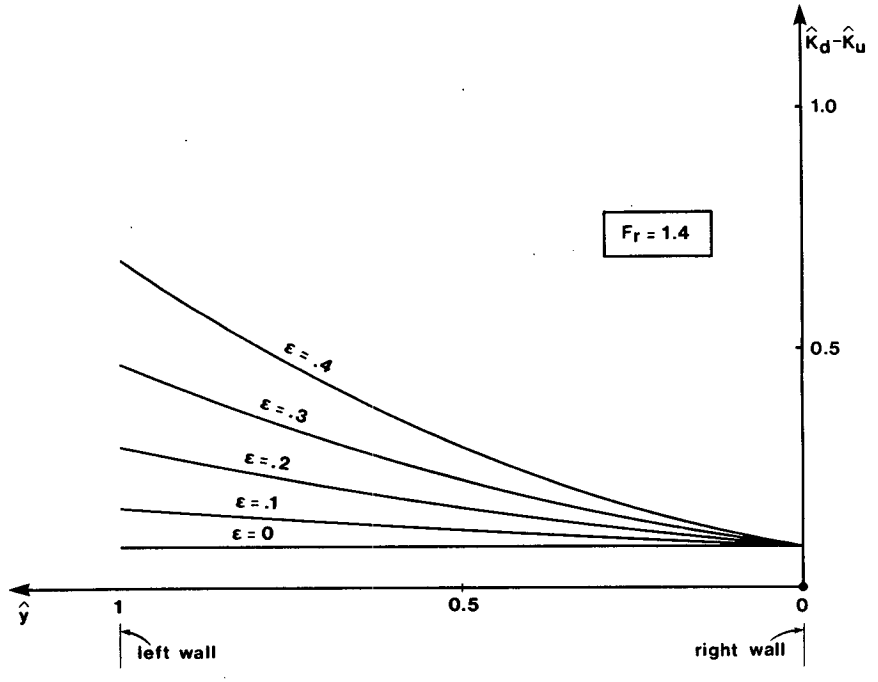

FIG. 9. The dependence of the gain in potential vorticity across the shock ($\hat{K}_d - \hat{K}_u$) on the location and ϵ. Note that ϵ represents the channel width (b/R_d). Also, note that the largest gain is on the left-hand side (facing downstream) where the wave amplitude is the largest.

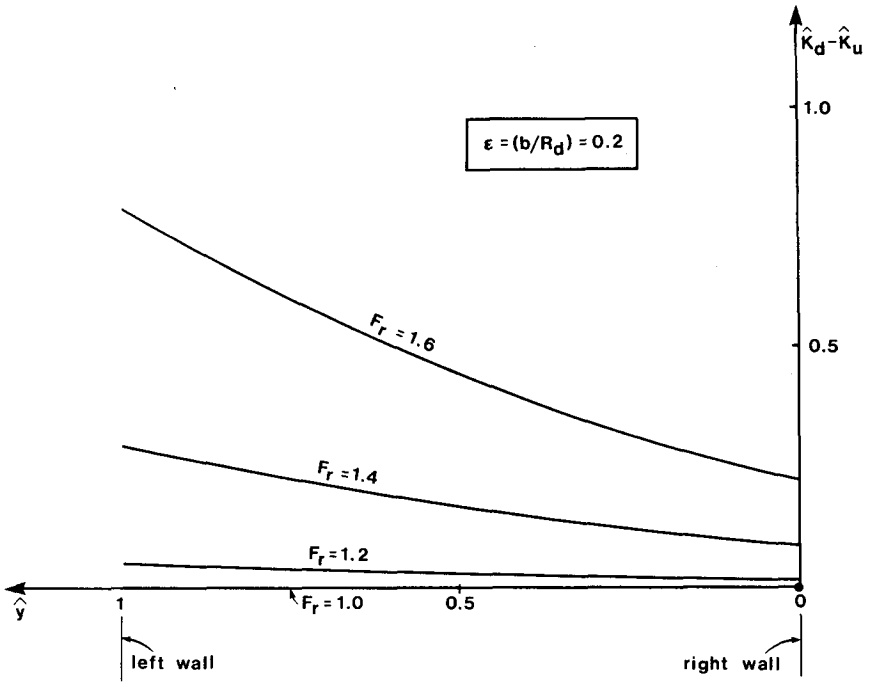

FIG. 10. The dependence of the gain in potential vorticity across the shock ($\hat{K}_d - \hat{K}_u$) on the location and Froude number.

waves whose amplitude is of the same order as the mean flow) the gain in potential vorticity is high [O(1)]. On the other hand, when the shock is weak [i.e., the ratio between the shock's amplitude and the mean depth (δ) is much smaller than unity ($\delta \ll 1$)], the change in potential vorticity is negligible [$O(\delta^2)$]. Note that Pratt's (1983) numerical simulations have also shown a gain in potential vorticity across a shock wave in a channel. The changes that he observed, however, were rather small, perhaps due to cross-channel flows which prevented the establishment of a purely geostrophic flow.

Although our solutions are particular in the sense that they do not represent the entire family of solutions for shock waves in a channel, they do show that shock waves are likely to occur in the ocean. In many straits and outflows, the internal Froude number easily ex-

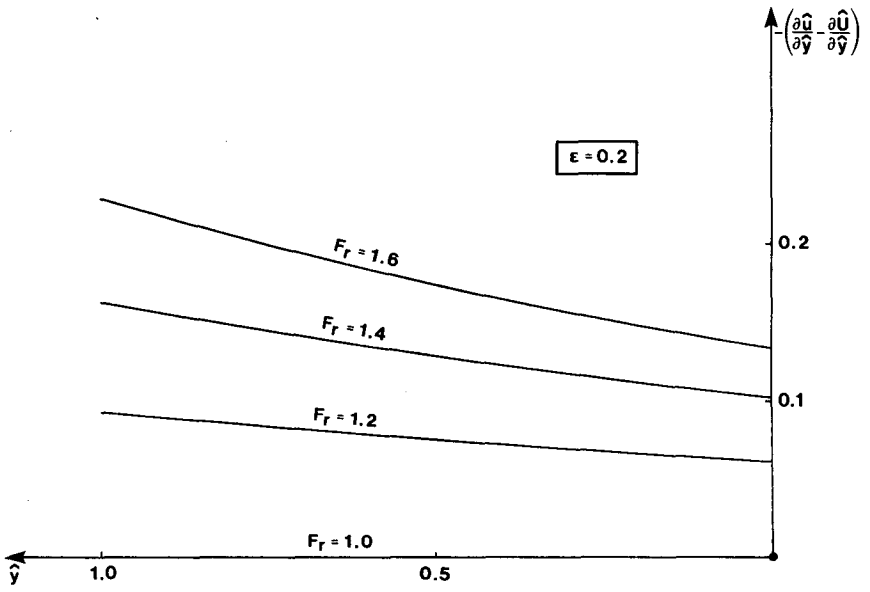

FIG. 11. The decrease in shear across the shock as a function of location and Froude number.

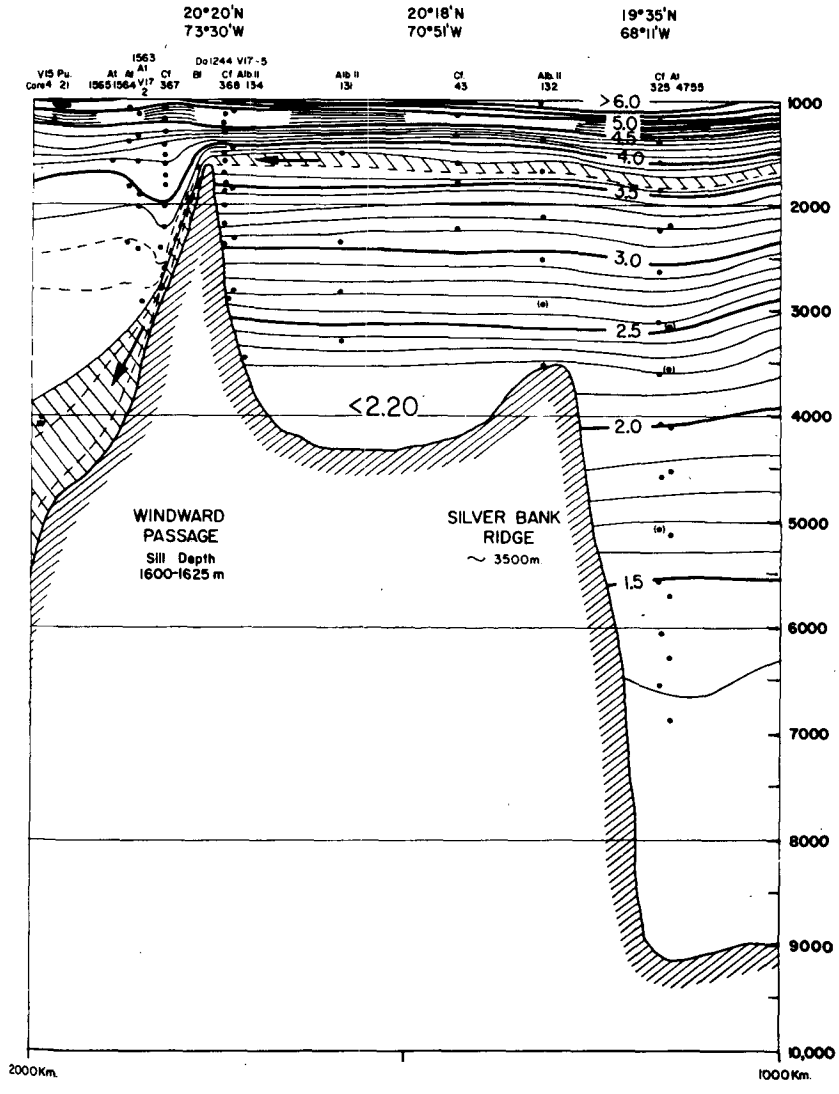

FIG. 12. The potential temperature structure in the Windward Passage and its vicinity (adapted from Wüst, 1964). Note that, in the lee of the sill, the deep water (i.e., the 4° isotherm) displays a jump similar to that suggested by our study (Figs. 2 and 4). Namely, the deep water (i.e., water with a potential temperature less than 4°) is flowing from right to left underneath a very deep upper layer which, as a first approximation, can be assumed to be at rest. To the left of the sill in the Windward Passage, the 4° isotherm initially deepens following the bottom slope. Near station Crawford 367 it abruptly rises, creating a structure that resembles a jump. It is important to realize, however, that the data for the region where the jump occurs were collected in two different cruises and, hence, should be interpreted with caution. It is believed, however, that while some small details in the area may differ from the displayed features, the actual basic pattern is probably valid because the displayed jump is relatively large (~800 m).

ceeds unity because the flows are shallow [~O(10 m)] and relatively fast [O(10–100 cm s^{-1})] so that shocks are certainly possible. For example, it appears from the analysis of Hogg (1983), Schmitz and Hogg (1983), and Hogg et al. (1982) that in the Vema Channel there is a transition from a supercritical flow to subcritical flow and this transition could include a shock. In addition, as mentioned in the Introduction, the cross section of the deep flow through the Denmark Strait shows a sudden jump in the interface depth, and this may be related to a shock (see Bainbridge 1976, p. 9). Figure 12 displays a cross section of the deep flow through the Windward Passage, and it appears that this flow may also contain a jump. Because of the limited number of observations available today and the lack of a more general solution for shock waves in a channel, a detailed quantitative comparison between our theory and observations is impossible at this stage.

Acknowledgments. This study was supported by the Office of Naval Research contract N00014-82-C-0404. Much of the calculations and plots were made with

the aid of Steve Van Gorder, whose help as a programmer is much appreciated. In particular, the derivation of the one-dimensional solution in its special form is largely due to his mathematical skills. Discussions with G. Weatherly regarding the observational aspects of the problem were very helpful. The comments of two anonymous reviewers as well as those of Larry Pratt (on an earlier version of this paper) were very helpful.

APPENDIX

Relationship to Previous Work

The following discussion addresses the relationship between the present study and the separated shock reported in Nof (1984); in particular, new questions regarding the closure condition used in Nof (1984) and the associated issue of "upstream influence" are addressed.

The fact that our analytical solutions show that across the shock there is an O(1) jump in the potential vorticity (Figs. 9 and 10) suggests that the closure condition used by Yamagata (1980) and Nof (1984) should be reexamined. This closure condition is based on the assumption that the potential vorticity is conserved across the shock. Specifically, Nof's closure condition is based on the idea that, because of the absence of a wall on the left-hand side (looking downstream), there

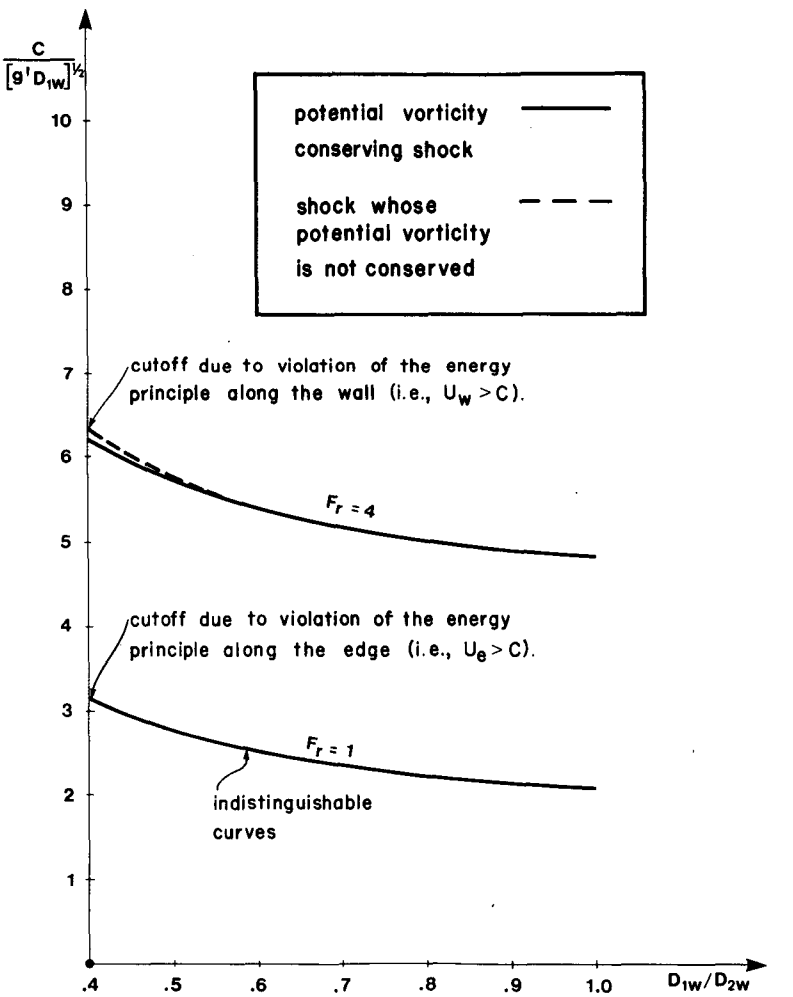

FIG. 13. The sensitivity of the separated shock propagation speed (C) to the potential vorticity distribution on the two sides of the shock, the Froude number, and the relative depth increase. The notation is identical to that used in Nof (1984), i.e., D_{1w} and D_{2w} are the conjugate depths near the wall, and U_w and U_e are the initial speeds at the wall and edge, respectively. The solid curves correspond to the predicted shock speed based on the closure condition, which assumes conservation of potential vorticity, whereas the dashed curves are based on continuous energy along the edge ($h = 0$) and a linear velocity profile which implies a discontinuous potential vorticity. Note that the two situations correspond to quite different velocity and potential vorticity profiles. In the former case (i.e., the solid curve), the velocity increases toward the left, whereas in the latter case (dashed line), the speed increases toward the right. Despite these major differences, the predicted speeds are extremely close to each other.

are no waves which can propagate upstream and, therefore, there is no "upstream influence." It has been argued that, consequently, the potential vorticity at the *source* cannot be changed and the final result is that the two fluids on the two sides of the propagating shock should have identical potential vorticities [see Fig. 4 in Nof (1984) and the associated discussion on p. 1690].

As already pointed out, there are important differences between the separated case and the channel case considered in this study, so the result of one study cannot be directly applied to the other. However, since it had never been independently established that the potential vorticity is indeed conserved in the separated current, the change of potential vorticity found in the channel case suggests that such a change can also be present in the separated case. At the time when the Nof (1984) paper was written, it was difficult to conceive a separated shock with an altered potential vorticity because such a situation implies that some disturbances will propagate upstream and we know that Kelvin waves cannot propagate without a wall on their right. Very recently, however, Kubokawa and Hanawa (1984) have discovered a new kind of wave which they call a "frontal wave"; this is a wave that can propagate *upstream* even though there is no wall on its right-hand side. The fact that such a wave can exist suggests that the upstream conditions of the separated current could indeed be altered. It implies that the potential vorticity could be modified at the source or, equivalently, the closure conditions used by Nof (1984) may not be adequate. An unequivocal answer to this question can only be given once a complete, detailed solution for the entire field can be obtained, and this is beyond the scope of this study.

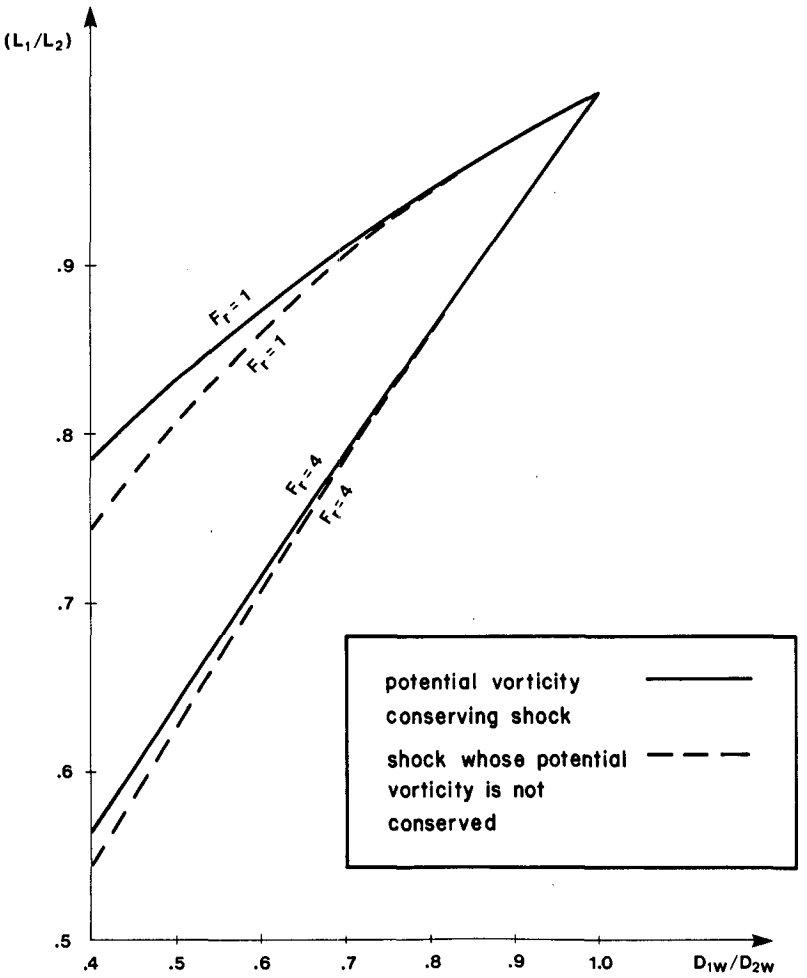

FIG. 14. The sensitivity of the separated shock increase in width (L_2/L_1) to (i) the potential vorticity distribution on the two sides of the shock, (ii) the Froude number, and (iii) the relative depth increase. As in Fig. 13, the solid curves correspond to a computation based on the Nof (1984) closure condition, which implies conservation of potential vorticity, whereas the dashed curves are based on a continuous energy along the edge ($h = 0$) and a linear velocity profile, which imply a discontinuous potential vorticity. Note that the differences between the results of the two methods of prediction are rather small.

It is important to note that, from a practical point of view, there is almost no difference between the Nof (1984) predictions (which are based on conservation of potential vorticity) and predictions which take into account entirely different distributions of potential vorticity on the two sides of the jump (Figs. 13 and 14). This results from the fact that the Nof (1984) computational techniques involve integrated quantities and these are very insensitive to the distribution of potential vorticity.

It should also be mentioned that the possible modification of potential vorticity in the separated current may help to explain an additional question regarding the Nof (1984) study. This question is related to the fact that, according to the Nof (1984) analysis and the conservation of zero potential vorticity across the shock, the energy loss along the current edge ($h = 0$) is finite, even though the Bernoulli principle [see Eq. (2.28) p. 1689] suggests that there should not be any energy loss along the edge. It has been previously assumed that these two, apparently contradictory, statements are a result of a singularity along the edge. However, our new study, and the Kubokawa and Hanawa study, suggest that a different situation is also possible. Specifically, the new considerations suggest the possibility that, along the edge, energy is conserved, whereas the zero potential vorticity is the one that is altered. As pointed out earlier, such questions can only be answered by solving for the entire field, which is beyond the scope of this study.

REFERENCES

Armi, L., and D. Farmer, 1985: The internal hydraulics of the Strait of Gibraltar and associated sills and narrows. *Oceanol. Acta,* **8,** 37–46.

Bainbridge, A. E., 1976: *Geosecs Atlantic Expedition, Vol. 2. Sections and Profiles.* U.S. Govt. Printing Office, Washington, DC, 198 pp.

Courant, R., and K. O. Friedrichs, 1948: *Supersonic Flow and Shock Waves.* Springer-Verlag, 464 pp.

Gill, A. E., 1977: The hydraulics of rotating-channel flow. *J. Fluid Mech.,* **80,** 641–677.

Hogg, N. G., 1983: Hydraulic control and flow separation in a multilayered fluid with applications to the Vema Channel. *J. Phys. Oceanogr.,* **13,** 695–708.

——, P. Biscaye, W. Gardner and W. J. Schmitz, Jr., 1982: On the transport and modification of Antarctic bottom water in the Vema Channel. *J. Mar. Res.,* **40,** 231–263.

Houghton, D. D., 1969: Effect of rotation on the formation of hydraulic jumps. *J. Geophys. Res.,* **74,** 1351–1360.

——, and A. Kasahara, 1968: Nonlinear shallow fluid over an isolated ridge. *Common. Pure Appl. Math.,* **21,** 1–23.

Kubokawa, A., and K. Hanawa, 1984: A theory of semigeostrophic gravity waves and its application to the intrusion of a density current along a coast. Parts I and II. *J. Oceanogr. Soc. Japan,* **40,** 247–270.

Lighthill, J., 1978: *Waves in Fluids.* Cambridge University Press, 504 pp.

Nof, D., 1984: Shock waves in currents and outflows. *J. Phys. Oceanogr.,* **14,** 1683–1702.

Parrett, C. A., and M. J. P. Cullen, 1984: Simulation of hydraulic jumps in the presence of rotation and mountains. *Quart. J. Roy. Meteor. Soc.,* **110,** 147–165.

Pratt, L. J., 1983: On inertial flow over topography. Part I. Semigeostropic adjustment to an obstacle. *J. Fluid Mech.,* **131,** 195–218.

Schmitz, W. J., Jr., and N. G. Hogg, 1983: Exploratory observations of abyssal currents in the South Atlantic near Vema Channel. *J. Mar. Res.,* **41,** 487–510.

Stoker, J. J., 1957: The formation of breakers and bores. *Commun. Pure Appl. Math.,* **1,** 1–87.

Williams, R. T., and A. M. Hori, 1970: Formation of hydraulic jumps in a rotating system. *J. Geophys. Res.,* **75,** 2813–2819.

Wüst, G., 1964: *Stratification and Circulation of the Antilles and Caribbean Sea Basins.* Columbia University Press, 201 pp.

Yamagata, T., 1980: A theory for propagation of an oceanic warm front with application to Sagami Bay. *Tellus,* **32,** 73–76.